Andrew Q. Tan, Ph.D.
Harvard Medical School
Boston, Massachusetts
and
Spaulding Rehabilitation Hospital
Boston, Massachusetts

Megan Hermann, P.T., D.P.T.
Arun Jayaraman, P.T., Ph.D.
Shirley Ryan AbilityLab
Chicago, Illinois

Victoria Stahl, Ph.D.
Emory University School of Medicine
Atlanta, Georgia

William Zev Rymer, M.D., Ph.D.
Shirley Ryan AbilityLab
Chicago, Illinois

Gordon S. Mitchell, Ph.D.
University of Florida
Gainesville, Florida

Heather B. Hayes, Ph.D.
Emory University School of Medicine
Atlanta, Georgia

Randy D. Trumbower, P.T., Ph.D.
Harvard Medical School
Boston, Massachusetts
and
Spaulding Rehabilitation Hospital
Boston, Massachusetts

ORCID IDs: 0000-0002-5201-8603 (I.V.); 0000-0002-2282-9974 (R.D.T.).

*Corresponding author (e-mail: ivivodtzev@partners.org).

References

1. Trumbower RD, Jayaraman A, Mitchell GS, Rymer WZ. Exposure to acute intermittent hypoxia augments somatic motor function in humans with incomplete spinal cord injury. *Neurorehabil Neural Repair* 2012;26:163–172.
2. Hayes HB, Jayaraman A, Herrmann M, Mitchell GS, Rymer WZ, Trumbower RD. Daily intermittent hypoxia enhances walking after chronic spinal cord injury: a randomized trial. *Neurology* 2014;82: 104–113.
3. Trumbower RD, Hayes HB, Mitchell GS, Wolf SL, Stahl VA. Effects of acute intermittent hypoxia on hand use after spinal cord trauma: a preliminary study. *Neurology* 2017;89:1904–1907.
4. Fields DP, Mitchell GS. Spinal metaplasticity in respiratory motor control. *Front Neural Circuits* 2015;9:2.
5. Huxtable AG, Smith SM, Peterson TJ, Watters JJ, Mitchell GS. Intermittent hypoxia-induced spinal inflammation impairs respiratory motor plasticity by a spinal p38 MAP kinase-dependent mechanism. *J Neurosci* 2015;35:6871–6880.
6. Sankari A, Vaughan S, Bascom A, Martin JL, Badr MS. Sleep-disordered breathing and spinal cord injury: a state-of-the-art review. *Chest* 2019; 155:438–445.
7. Cohen J. Statistical power analysis for the behavioral sciences. New York, NY: Lawrence Erlbaum Associates; 1988.
8. Peng YJ, Overholt JL, Kline D, Kumar GK, Prabhakar NR. Induction of sensory long-term facilitation in the carotid body by intermittent hypoxia: implications for recurrent apneas. *Proc Natl Acad Sci USA* 2003;100:10073–10078.
9. Lovett-Barr MR, Satriotomo I, Muir GD, Wilkerson JE, Hoffman MS, Vinit S, *et al*. Repetitive intermittent hypoxia induces respiratory and somatic motor recovery after chronic cervical spinal injury. *J Neurosci* 2012;32:3591–3600.
10. Navarrete-Opazo A, Alcayaga J, Sepúlveda O, Rojas E, Astudillo C. Repetitive intermittent hypoxia and locomotor training enhances walking function in incomplete spinal cord injury subjects: a randomized, triple-blind, placebo-controlled clinical trial. *J Neurotrauma* 2017;34:1803–1812.

A Unique Case of Secondary Pulmonary Alveolar Proteinosis after E-Cigarette, or Vaping, Product Use–associated Lung Injury

To the Editor:

Clinical, radiographic, and histopathologic criteria continue to emerge in cases of e-cigarette, or vaping, product use–associated lung illness (EVALI) (1, 2). We report a unique case of EVALI with radiographic, cytologic, and electron microscopy (EM) findings most consistent with secondary pulmonary alveolar proteinosis (PAP).

A 20-year-old female patient with chronic tetrahydrocannabinol (THC) vape use presented to the emergency room with 10 days of progressive dyspnea and cough. Her past medical history was significant for major depressive and anxiety disorder since 2015. She had no prior medical history of recurrent respiratory symptoms or prior diagnosis of chronic respiratory disease. She admitted to vaping counterfeit THC-based e-cigarette cartridges daily (50–100 puffs/d) for over a year. More specifically, she admitted purchasing THC-based cartridges from a friend that often did not have standardized labeling, strongly suggestive of noncertified or counterfeit production. She also reported inhaling marijuana using a water pipe with "dabs" on a bong nail as well as regular alcohol use (1–2 drinks

Table 1. Laboratory Workup at Initial Presentation

Laboratory Test	Result	Reference Values
CRP, mg/L	178	0–10
ESR, mm/h	70	0–20
LD, U/L	904	118–225
Platelets, $\times 10^9$/L	377	160–370
WBC, $\times 10^9$/L	20.9	4.0–10.0
Neutrophils, $\times$1,000/μl	18.2	1.6–6.1
Lymphocytes, $\times$1,000/μl	1.3	1.2–3.7
Hb, g/dl	10.7	11.2–15.7
Hct, %	33	34–45
BUN, mg/dl	12	6–20
Creatinine, mg/dl	0.5	0.5–1.0
Sodium, mmol/L	134	133–145
Postassium, mmol/L	2.9	3.3–5.1
Chloride, mmol/L	94	96–108
Cultures	Negative	NA

Definition of abbreviations: BUN = blood urea nitrogen; CRP = C-reactive protein; ESR = erythrocyte sedimentation rate; Hct = hematocrit; LD = lactate dehydrogenase; NA = not applicable; WBC = white blood cell count.

Originally Published in Press as DOI: 10.1164/rccm.202002-0252LE on May 11, 2020

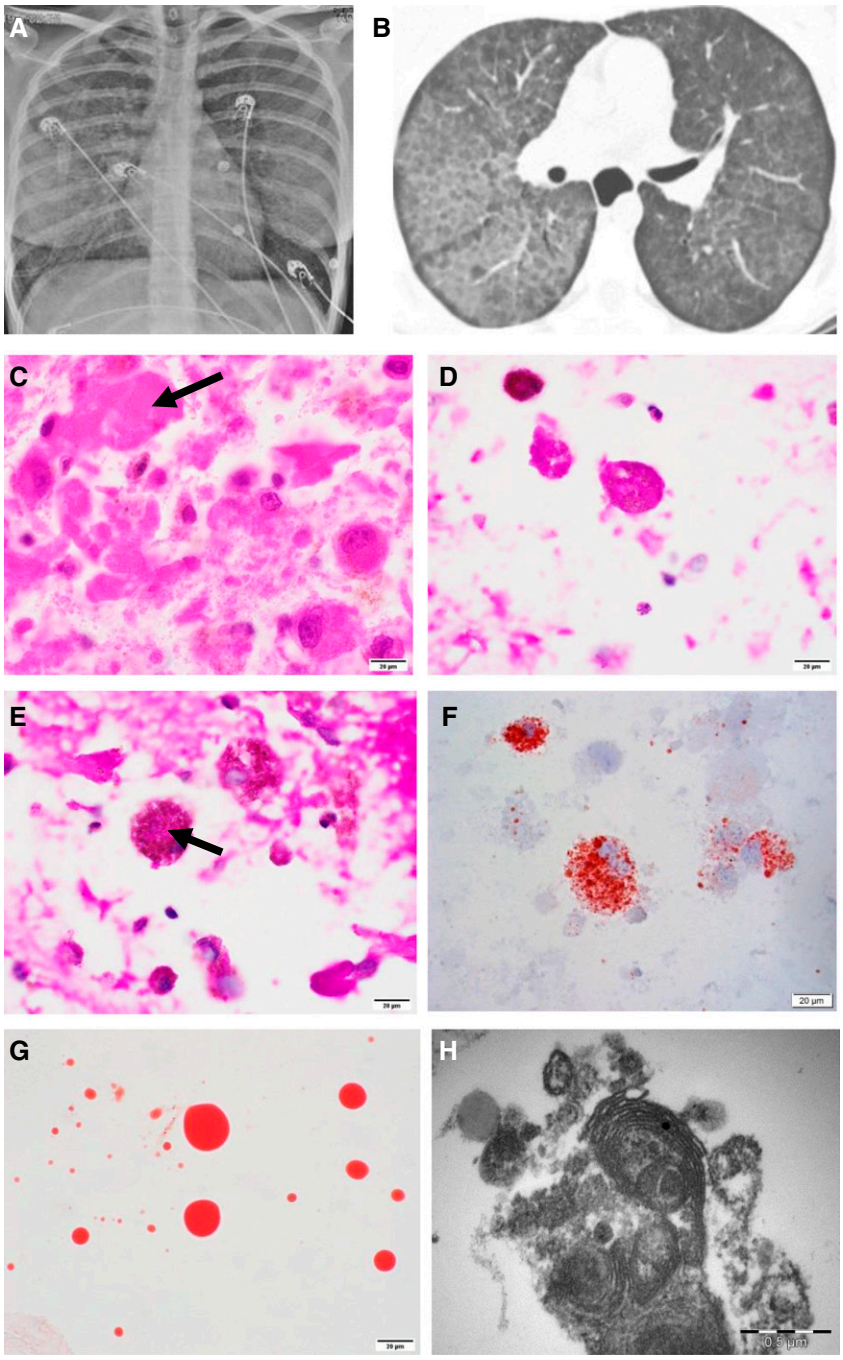

Figure 1. (*A*) Frontal chest X-ray with bilateral perihilar hazy air space opacification. (*B*) High-resolution chest computed tomographic scan showing interlobular septal thickening forming a crazy paving pattern. (*C*) Hematoxylin and eosin showing extracellular eosinophilic hyaline material (arrow). (*D*) Periodic acid–Schiff with diastase–positive extracellular globular material. (*E*) Periodic acid–Schiff with diastase–positive granular deposit in intracytoplasmic macrophages (arrow). (*F*) Oil red O stain highlighting intracytoplasmic (macrophages) lipid vacuoles. (*G*) Oil red O stain–positive extracellular hyaline globules. (*C*–*G*) Scale bars, 20 μm. (*H*) Electron microscopy showing myelin-like whorled membranous structures (lamellar bodies) (scale bar, 0.5 μm).

per evening) but denied combustible cigarette, smokeless tobacco, or other illicit drug use.

On presentation, her physical exam was significant for hypoxemia, tachypnea, fever, and bilateral lower lobe inspiratory crackles. Her laboratory evaluation revealed leukocytosis with significant neutrophilia and elevated inflammatory markers, but microbiologic culture studies were negative, ruling out infectious etiology (Table 1). Chest X-ray showed bilateral diffuse interstitial opacities. A high-resolution computerized tomographic imaging of the chest demonstrated diffuse bilateral ground glass opacities with

subpleural sparing and associated septal thickening, consistent with "crazy paving" (Figures 1A and 1B).

After admission for noninvasive respiratory support and oxygen supplementation, BAL was performed. BAL cytology showed a neutrophilic infiltrate with numerous foamy macrophages and extracellular granular to globular material in the background. Subsequent Oil red O (ORO) staining showed intracytoplasmic (macrophages) lipid deposition. Periodic acid–Schiff with diastase (PAS-D) was positive for extracellular and amorphous eosinophilic material within the macrophages. Extracellular hyaline globules stained with ORO were also noted. EM showed characteristic lamellar bodies, representing surfactant (*see* Figures 1C–1H). The patient improved after treatment with antibiotics and steroids, independent of therapeutic whole lung lavage. She was subsequently discharged home, vowing to discontinue vaping.

The radiographic, cytologic, and EM findings (crazy paving, PAS and PAS-D–positive material, and lamellar bodies) are unique in this case of EVALI and have not been previously described. Furthermore, they are most consistent with secondary PAP (3, 4).

Prior case reports of EVALI demonstrate similar clinical presentation and serologic evaluation as the case presented here with dyspnea, hypoxemia, leukocytosis with neutrophilic predominance, and prominent inflammatory markers in the absence of an identifiable infectious cause (5, 6). In addition, our patient showed an elevated lactate dehydrogenase level, which is a nonspecific finding but often present in PAP. Other routine laboratory tests are usually normal in PAP (3).

Radiographically, EVALI presents with a variety of patterns and commonly shows bilateral opacities with subpleural sparing. EVALI may mimic other conditions radiographically, such as hypersensitivity pneumonitis, diffuse alveolar hemorrhage, acute eosinophilic pneumonia, diffuse alveolar damage, organizing pneumonia (OP), lipoid pneumonia, and giant cell interstitial pneumonia (4). PAP is commonly associated with bilateral symmetrical or patchy ground glass opacities, often with mid to lower lung predominance, and with septal thickening, which is also known as crazy paving (3).

A variety of histologic findings have been described in EVALI, including diffuse alveolar damage, OP, and acute fibrinous OP (7, 8). Accumulation of ORO stain–positive macrophages is a well-known, albeit nonspecific, feature of EVALI (8). PAS and PAS-D–positive material and macrophages, as well as lamellar bodies on EM, have not been described in other cases of EVALI and are more commonly associated with PAP. On routine histologic exam, PAP shows well-preserved alveoli filled with granular, eosinophilic, PAS-D–positive material, and minimal associated interstitial inflammation and fibrosis (3).

The vast majority of PAP cases are related to anti–granulocyte–macrophage colony–stimulating factor autoantibodies (primary PAP). Approximately 8% to 9% of PAP cases are classified as secondary, due to underlying conditions such as hematologic diseases, nonhematologic malignancies, immune deficiencies, chronic infection or inflammation, and toxic inhalation exposure. Common treatment for primary PAP is whole lung lavage and high-dose steroids. Conversely, treatment for secondary PAP is treatment of the underlying cause (3). Similar to other cases of EVALI, the patient presented in this case report responded to steroid treatment, forgoing the need for whole lung lavage, which further supports a diagnosis of secondary PAP (3, 9).

Pathogenesis of secondary PAP is thought to be due to impaired alveolar macrophage number or function, including surfactant catabolism (3). Recently, alterations in lung lipid homeostasis with aberrant phospholipids in alveolar macrophages and increased surfactant-associated phospholipids were described in a mouse model of chronic e-cigarette exposure (10). We hypothesize EVALI may represent a severe form of macrophage dysfunction, with subsequent surfactant accumulation in the alveolar spaces and secondary pulmonary proteinosis development. Considering that most patients with EVALI do not present with secondary PAP, further testing is required in eliciting the underling mechanism of EVALI pathogenesis and for identifying susceptible populations more prone to e-cigarette– or vaping-associated lung injury. ■

Author disclosures are available with the text of this letter at www.atsjournals.org.

Acknowledgment: The authors thank Karen Bentley and Karen Vanderbilt of the Electron Microscopy Core Facility at the University of Rochester Medical Center for technical assistance.

Anna-Karoline Israel, M.D.
Moises J. Velez, M.D.
Serban A. Staicu, M.D.
Robert Ambrosini, M.D., Ph.D.
Matthew McGraw, M.D.
Tanupriya Agrawal, M.D., Ph.D.*‡
University of Rochester Medical Center
Rochester, New York

ORCID IDs: 0000-0002-5646-3560 (M.M.); 0000-0002-7649-2828 (T.A.).

*Present address: University of Rochester Medical Center, Rochester, New York.
‡Corresponding author (e-mail: tanupriya_agrawal@urmc.rochester.edu).

References

1. Zou RH, Tiberio PJ, Triantafyllou GA, Lamberty PE, Lynch MJ, Kreit JW, *et al*. Clinical characterization of e-cigarette, or vaping, product use associated lung injury in 36 patients in Pittsburgh, Pennsylvania. *Am J Respir Crit Care Med* 2020;201:1303–1306.
2. Layden JE, Ghinai I, Pray I, Kimball A, Layer M, Tenforde MW, *et al*. Pulmonary illness related to E-cigarette use in Illinois and Wisconsin - final report. *N Engl J Med* 2020;382:903–916.
3. Suzuki T, Trapnell BC. Pulmonary alveolar proteinosis syndrome. *Clin Chest Med* 2016;37:431–440.
4. Henry TS, Kligerman SJ, Raptis CA, Mann H, Sechrist JW, Kanne JP. Imaging findings of vaping-associated lung injury. *AJR Am J Roentgenol* 2020;214:498–505.
5. Triantafyllou GA, Tiberio PJ, Zou RH, Lamberty PE, Lynch MJ, Kreit JW, *et al*. Vaping-associated acute lung injury: a case series. *Am J Respir Crit Care Med* 2019;200:1430–1431.
6. Boloña E, Felix M, Vanegas E, Vera Paz C, Cherrez-Ojeda I. A case of vaping-associated pulmonary illness in South America: highlighting the need for awareness and surveillance programs in the region. *Am J Respir Crit Care Med* 2020;201:733–735.
7. Lu MA, Jabre NA, Mogayzel PJ Jr. Vaping-related lung injury in an adolescent. *Am J Respir Crit Care Med* 2020;201:481–482.
8. Mukhopadhyay S, Mehrad M, Dammert P, Arrossi AV, Sarda R, Brenner DS, *et al*. Lung biopsy findings in severe pulmonary illness associated with e-cigarette use (vaping). *Am J Clin Pathol* 2020;153: 30–39.
9. Alzghoul BN, Innabi A, Mukhtar F, Jantz MA. Rapid resolution of severe vaping induced acute lipoid pneumonia following corticosteroid treatment. *Am J Respir Crit Care Med* [online ahead of print] 6 Mar 2020; DOI: 10.1164/rccm.201909-1826IM.

10. Madison MC, Landers CT, Gu B-H, Chang C-Y, Tung H-Y, You R, *et al*. Electronic cigarettes disrupt lung lipid homeostasis and innate immunity independent of nicotine. *J Clin Invest* 2019;129: 4290–4304.

Successful Treatment of Interstitial Lung Disease in STAT3 Gain-of-Function Using JAK Inhibitors

To the Editor:

Germline, gain-of-function (GOF) mutations in *STAT3* (signal transducer and activator of transcription 3) cause an autosomal dominant inborn error of immunity (1, 2). STAT3 is a transcription factor activated by JAKs (Janus kinases) after upstream receptor ligation from various cytokines, including IL-6. STAT3 is involved in multiple processes, including critical roles in immunity and inflammation. Therefore, STAT3 GOF leads to an early-onset disease with varied phenotypes, including immune-mediated cytopenias, solid organ autoimmunity, lymphoproliferation, severe growth restriction, and hypogammaglobulinemia with recurrent infections (3). Interstitial lung disease (ILD) affects nearly 40% of patients, usually developing during the second decade (3–5). After hematologic features, growth restriction, and gastrointestinal manifestations, lung disease is the fourth most frequent aspect of this disease (3).

Before the discovery of STAT3 GOF syndrome, patients with STAT3 GOF were treated with years of highly immunosuppressive therapy in attempts to control disease manifestations (2). However, there are now targeted biotherapies against cytokine signaling pathways. These include anti–IL-6 receptor monoclonal antibody therapy (tocilizumab and sarilumab), currently approved for indications such as rheumatoid arthritis and juvenile arthritis (6), and JAK inhibitors (ruxolitinib, baricitinib, tofacitinib, and upadacitinib), collectively approved for a variety of indications, including rheumatoid arthritis and ulcerative colitis (7). Using these targeted biotherapies as the first line in STAT3 GOF syndrome provides an opportunity to optimize treatment efficacy while minimizing side effects. The first international cohort describing the use of JAK/STAT–targeted therapies in STAT3 GOF showed encouraging results for the treatment of immune dysregulation, particularly when introduced early in the course of disease (8).

Indication, dose, and efficacy of JAK inhibitors in STAT3 GOF syndrome–induced ILD has not yet been established. We aimed to comprehensively describe the first available pulmonary data on use of JAK inhibitors in STAT3 GOF patients with ILD. Some of these results have been previously reported in the form of an abstract (9).

Methods

Consent to report patient data was obtained in accordance with internal review board and ethics committee requirements. Patients at two tertiary pulmonary referral centers with functionally confirmed GOF *STAT3* mutations were included if treated with a JAK inhibitor. Type of ILD, BAL findings, pathology, pulmonary function tests, computed tomographic (CT) scan results, type of respiratory support, and outcomes were assessed for available patients before treatment and at last follow-up. Results are expressed as median (interquartile range).

Results

Detailed information was available for four patients with STAT3 GOF with ILD (two French and two at Texas Children's Hospital) treated with JAK inhibitors, two with ruxolitinib and two with tofacitinib (Table 1). At diagnosis, the four patients had clubbing, three had tachypnea, and one had crackles. One patient required oxygen support alone and one patient required oxygen with continuous noninvasive ventilatory support with bilevel positive pressure. CT scans showed ground-glass opacities in all patients, septal thickening in two, and architectural distortion in two. BAL fluid analysis was available for three patients showing hypercellularity, and significant lymphocytosis in patient 2 (69%). Lung biopsy was performed in three patients, with inconclusive results in one and findings consistent with lymphocytic interstitial pneumonia (LIP) and nonspecific interstitial pneumonia in the other two patients. Pulmonary function testing showed restriction in one patient and a diffusion defect in two others. Overall, the final radiologic, BAL, and biopsy results led to the diagnosis of LIP in two cases, desquamative interstitial pneumonia in one case, and nonspecific interstitial pneumonia in one case (Table 1).

Initial nontargeted immunosuppressive therapies were used in three patients and were not effective in preventing onset of ILD or improving clinical symptoms or functional or radiologic assessments. Three patients had previously been treated with tocilizumab monotherapy for a median of 8 months (7.5–17). Unfortunately, tocilizumab monotherapy provided insufficient improvement and, in one case, no improvement, in respiratory status. This led to the introduction of a JAK inhibitor in addition to, or instead of, tocilizumab. Additionally, one patient was directly initiated on targeted therapy using a JAK inhibitor.

JAK inhibitor selection was based on availability and patient size. The two younger, smaller patients were started on ruxolitinib, which is available in multiple sizes, so the dose can be titrated more easily (8). Tofacitinib was selected for the two older patients, who both have concurrent arthritis. The median length of JAK inhibitor treatment was 21.5 months (18–29.25). Introduction of a JAK inhibitor led to complete discontinuation of oxygen and ventilatory support after 27 months in one patient and discontinuation of rest oxygen after 10 months in a second patient. Clinical exam improved in all patients. Serial chest CT scans revealed stable cystic changes

Author Contributions: M.S.-C., T.P.V., L.R.F., and L.G.-C. drafted the initial manuscript, participated in the conceptualization and design of the study, contributed to the acquisition of data, performed a complete review of the current literature, critically revised the manuscript, and approved the final manuscript as submitted. S.M., J.-C.D., S.L., A.F., and V.B. were involved in clinical follow-up of the patients, participated in the conceptualization and design of the study, contributed to the acquisition of data, critically revised the manuscript, and approved the final manuscript as submitted. M.G. participated in the conceptualization and design of the case report, contributed to the acquisition of the computed tomographic scans, critically revised the manuscript, and approved the final manuscript as submitted.

Originally Published in Press as DOI: 10.1164/rccm.201906-1204LE on May 11, 2020